Analytical Characterization of unipolar diode based on Transistor Channels model

Fatima Zohra Mahi, A. Majid. Mammeri
Institute of Science and Technology
university of Bechar
Algeria
fati_zo_mahi2002@yahoo.fr

H. Marinchio, C. Palermo and L. Varani
Institute of electronic and systems
university of Montpellier 2
France
fati64@live.com

Abstract: In this paper, we propose an analytical approach for the small-signal response of nanometric InGaAs diode which is extracted to the transistor model in ref [1] when the gate is taking away. The exploitation of the small-signal equivalent circuit elements such as the admittance parameters can give significant information about the noise level of the devices by using the Nyquist relation. The analytical model takes into account the longitudinal and the transverse electric fields through a pseudo two-dimensional approximation of the Poisson equation. For the transistor, the total currents -potentials matrix relation between the gate and the drain terminals determine the frequency-dependent of the small-signal admittance response. The noise calculated by using the real part of the transistor/diode admittance under a small-signal perturbation. The results show that the admittance spectrum exhibits a series of resonant peaks corresponding to the excitation of plasma waves. The appearance of the resonance is discussed as functions of the device geometry (devices length) and the operating temperature. The model can be used, on one hand; to control the appearance of the plasma resonances, and on other hand; to determine the noise level of the InGaAs transistor and diode for the terahertz detection.

Key–Words: High mobility InGaAs transistors, nanometric diode, noise, Terahertz frequency

1 Introduction

In the last years, two devices such as the nanodiode and the transistor have shown a great potential application for the terahertz frequency range. As a new type, the InGaAs transistors (high mobility electrons transistors HEMT) have become interesting devices for terahertz (THz) applications as detectors and emitters working at room temperature [2]. In particular, the modern InGaAs transistors have emerged as important competitors due to the existence of THz plasma wave oscillations in the channel [3], [4]. In addition, the unipolar nanodiode has shown experimentally a good responsivity and noise properties for microwave and terahertz detection [5].

One of the most important microwave characterizations of HEMT transistors is based on the determination of the small-signal equivalent circuit elements such as the admittance parameters of their three-terminals. The analysis of the complex admittances provides important information about the high-frequency current noise of the transistors. The admittance studies can perform the dynamic regime of the electrons behavior under small-signal perturbation.

Moreover, when we increase the distance channel-gate the behavior of the transistor tends more and more to behave as a diode. This modification leads to obtain an ungated transistor, in other physical description; the device becomes a channel diode with two terminals (cathode and anode). In particular, the ungated transistor idea can over the parameters calculations aspect of unipolar diode. The small-signal diode investigation has directly obtained from the analytical transistor approach by considering a high distance value between the gate and the channel. More recently, the calculation of the admittance and the noise spectral density in the unipolar diode has useful to simulate the voltage oscillation [1] and to determine the minimum detectable power in terahertz radiations [5].

In this article, we present the small-signal admittance response and the noise spectrum calculation in InGaAs transistor and unipolar diode by using an analytical model. The analytical approach based on the linearization of Poisson equation, and applied to obtain the currents-voltages matrix relation describing the behavior of the devices in the terahertz frequency small-signal regime.
The matrix determines the admittance at the gate, drain and gate-drain terminals when the gate covers the total channel of transistor (for gated transistor). The parameters of the unipolar diode, noise and admittance, are determined by considering the channel-

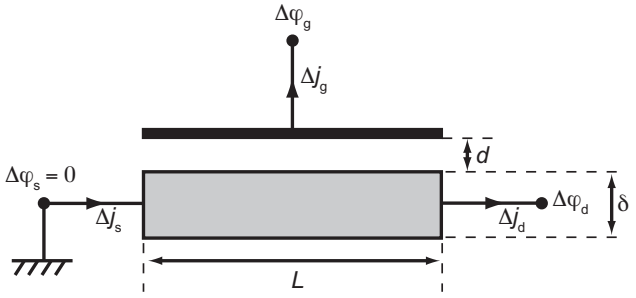

Figure 1: Structure representation of the field-effect transistor of channel length L, channel thickness δ and gate to channel distance d. $\Delta\varphi_d$, $\Delta\varphi_g$ and $\Delta\varphi_s$ are the amplitudes of the drain, gate and source oscillations, respectively.

gate distance tends to infinity (case of ungated transistor). In addition, the model uses the real part of the admittance and the Nyquist relation to determine the noise spectral density in the devices.

The article discussed the influence of the geometrical devices parameters (diode length or channel length) and the operating temperature on the admittance and electronic noise results. Moreover, the model gives a comparison between the resonances obtained by the diode and the transistor devices.

1.1 Response of High Mobility Transistor

In this section, we interest to evaluate the small-signal currents-voltages matrix for the HEMT transistors. The description of the transistor characterization is obtained by an analytical model under a continuous branching of the current between the channel and the gate.

We consider that the gate covers the total channel in the structure of figure 1.

The transistor structure is reported schematically in figure 1 where the channel is characterized by the length L and the thickness δ, d is the channel-gate distance, $\Delta\varphi_d$, $\Delta\varphi_g$ and $\Delta\varphi_s$ are the fluctuating voltages at the drain, the gate and the source respectively. In this approach, we assume that the channel is subdivided into n cells of length Δx connected in series and that the current flows along the channel in the one-dimensional direction (1D). In addition, the model takes into account the displacement currents which are described by the local capacitance between the channel and the gate, and considers the drift current only in the channel related to the carrier velocity (the vertical charge transport from the gate is absent). The voltage distribution along the channel $\Delta\varphi_x$ is described by a one-dimensional Poisson equation approximated as [6], [7]:

$$\frac{\partial^2}{\partial x^2}\Delta\varphi(x) + \lambda^2\left(\Delta\varphi_g - \Delta\varphi(x)\right) = -\frac{1}{\epsilon_c\epsilon_0}\rho^{3D}(x) \tag{1}$$

where $\lambda = \sqrt{\epsilon_d/\epsilon_c d\delta}$ is the plasma wavelength and $\epsilon_{c,d}$ is the dielectric constants in the channel and in the dielectric between the channel and the gate, respectively. For the equation (1) we take into consideration the potential boundary conditions $\Delta\varphi(x=0)$ and $\Delta\varphi(x=L)$ which are equals to $\Delta\varphi_s$ and $\Delta\varphi_d$, respectively [7]. By using the conservation law of the displacement and drift currents and going to the spectral representation, the charge density ρ^{3D} can be written as [7], [8]:

$$\rho^{3D} = -\frac{1}{i\omega}\frac{\partial}{\partial x}\Delta j_c^{drift}(x) \tag{2}$$

The drift current along the channel is obtained from the free carrier flow under an applied voltage as [4]:

$$\Delta j_c^{drift}(x) = -\epsilon_c\epsilon_0\frac{\omega_p^2}{i\omega+\nu}\frac{\partial}{\partial x}\Delta\varphi(x) \tag{3}$$

where $\omega_p = \sqrt{e^2 n_0/\epsilon_0\epsilon_c m^*}$ is the free-carrier 3D plasma frequency in the channel, ν is the relaxation rate and n_0 is the donor concentration in the channel.

By including equations (3) and (2) into equation (1), the voltage fluctuations in the channel are given by:

$$\frac{\partial^2}{\partial x^2}\Delta\varphi(x) + \beta^2\left(\Delta\varphi_g - \Delta\varphi(x)\right) = 0 \tag{4}$$

where $\beta^2 = \lambda^2\left[(i\omega(i\omega+\nu))/(\omega_p^2 + i\omega(i\omega+\nu))\right]$. The gate and channel currents are calculated from the potential $\Delta\varphi(x)$ which is obtained by a general solution of equation (4). Therefore, the solution of equation (4) is proportional to the homogeneous solution of second differential order equation.

The total current along the channel is determined by the displacement and drift current components [7], [8]:

$$\Delta j_c(x) = \left[-\epsilon_0\epsilon_c(i\omega)\frac{\partial}{\partial x}\Delta\varphi(x) + \Delta j_c^{drift}(x)\right] \tag{5}$$

The displacement and the drift currents are given by the first and the second terms of equation (5), respectively where the drift current is obtained by equation (3). In addition, the equation (5) can determine the current at the channel terminals, the drain and the source currents (Δj_d and Δj_s), which is given by Δj_d

and Δj_s corresponding to $x = L$ and $x = 0$ respectively.

The gate current equals to the displacement current as [3]:

$$\Delta j_g(x) = -\frac{\epsilon_d \epsilon_0}{d\delta} \int_0^L \frac{\partial}{\partial t} \left[\Delta\varphi_g - \Delta\varphi(x)\right] dx \quad (6)$$

By using equations (5) and (6), we obtain the currents-voltages relations at the drain-gate terminals which can be represented in a matrix form [9]:

$$\begin{bmatrix} \Delta j_d(\omega) \\ \Delta j_g(\omega) \end{bmatrix} = \begin{pmatrix} Y_{11} & Y_{12} \\ Y_{21} & Y_{22} \end{pmatrix} \begin{bmatrix} \Delta\varphi_d(\omega) \\ \Delta\varphi_g(\omega) \end{bmatrix} \quad (7)$$

The detailed expressions of the matrix elements are: $Y_{11} = \gamma \frac{cosh\beta L}{sinh\beta L}$, $Y_{12} = Y_{21} = \gamma \frac{(1-cosh\beta L)}{sinh\beta L}$, $Y_{22} = -2\gamma \frac{(1-cosh\beta L)}{sinh\beta L}$ where $\gamma = \epsilon_c \epsilon_0 \frac{\omega_p^2}{i\omega+\nu} \frac{\beta}{\alpha}$ and $\alpha = \omega_p^2 / \left[\omega_p^2 + i\omega\left(i\omega + \nu\right)\right]$. Here the elements Y_{ij} are the admittances of the drain, the drain-gate, the gate-drain and the gate for ij =11, 12, 21 and 22, respectively.

The source-drain matrix relation is obtained as

$$\begin{bmatrix} \Delta j_s(\omega) \\ \Delta j_d(\omega) \end{bmatrix} = \frac{\gamma}{sh\beta L} \begin{pmatrix} ch\beta L & -1 \\ 1 & -ch\beta L \end{pmatrix} \begin{bmatrix} \Delta\varphi_s(\omega) \\ \Delta\varphi_d(\omega) \end{bmatrix} \quad (8)$$

The equations (7) and (8) represent the analytical basis for the response characterization of the transistor. Therefore, we can obtain the related admittance to the plasma wave excitation in the terahertz frequency range. for the characterization of the transistor in small-signal regime, we calculate and discuss the modulus of the admittances at gate-drain terminals by using equation (7).

In other hand, for the unipolar diode characterization we evaluate the admittance at the drain-source terminals by using equation (8) and we consider high d value ($d \to \infty$).

2 Admittance Response of the Homogenous InGaAs Diode

Let us examine the modifications introduced by the gate-channel distance d in figure 1, when the gate is moved away from the channel the transistor behavior becomes more and more similar to that of the diode. Moreover, this consideration ($d \longrightarrow \infty$) leads to use the analytical model described in section 2 for the unipolar diode characterization. In absence of the gate, the transistor terminals : source, drain and gate corresponding to anode, cathode for the diode terminals, respectively. Therefore, the admittance terms of the diode are obtained by equation (8) where the matrix elements are simplified as: $\Delta j_s = Y_{anode} \Delta\varphi_s$ and $\Delta j_d = Y_{cathod} \Delta\varphi_d$. According to equation (8) the admittances of the anode and the cathode are simplified by $Y_{anode} = -Y_{cathode} = Y_{11}$.

3 Spectrum Noise

In the thermal equilibrium, the regular and spontaneous small-signal responses calculated, respectively, by the real part of admittance and the Nyquist relation as [9]:

$$\Delta S_{JJ}^{ij} = 4KTRe[Y_{ij}(\omega)] \quad (9)$$

The equation (9) can describe the spectral density of the current noise when we introduce the real part of the admittance.

4 Results and Discussion

In order to extract the admittance behavior, we consider an InGaAs transistor with channel length L = 400 nm, channel concentration $n_0 = 8 \times 10^{17}$ cm^3, thickness δ = 15 nm, distance channel-gate d = 10 nm and relaxation rate corresponding to room temperature $\nu = 3 \times 10^{12}$ s^1. For the diode calculations, we keep the same parameters as the transistor and we take the channelgate distance tends to infinity ($d \longrightarrow \infty$).

The results in this section present the frequency dependence of the admittance modulus $|Y_{ij}|$ in the InGaAs HEMT transistor and unipolar diode. We discuss only the admittance Y_{11} and Y_{12} spectrum since $Y_{12} = Y_{21} = -Y_{22}/2$ (see the detailed expressions of the matrix of equation (7)).

4.1 Transistor and Diode Admittance Comparison

Figure 2 shows the modulus of the admittance calculated for the transistor with d = 10 nm and for diode with $d \longrightarrow \infty$. We remark a series of resonance peaks (solid line) due to the thermal excitation of plasma waves. The resonance frequency positions can be calculated by the analytical expression $\omega_{res} = \omega_p k / \sqrt{(\lambda L/\pi)^2 + k}$ where k = 0, 1, 2, 3, 4... In particular, the admittance modulus $|Y_{11}|$ takes all the plasma resonance of fundamental excitation for k = 0, 1, 2, 3, 4 corresponding respectively to 1, 2, 2.7, 3.6, 4.3, 5, 5.6 and 6 THz. However, the resonance peaks of the $|Y_{12}|$ admittances present only the odd resonance corresponding to k = 1, 3, 5, 7.... Therefore, the drain terminal stimulation can excite all plasma modes (see spectrum), on the contrary, a

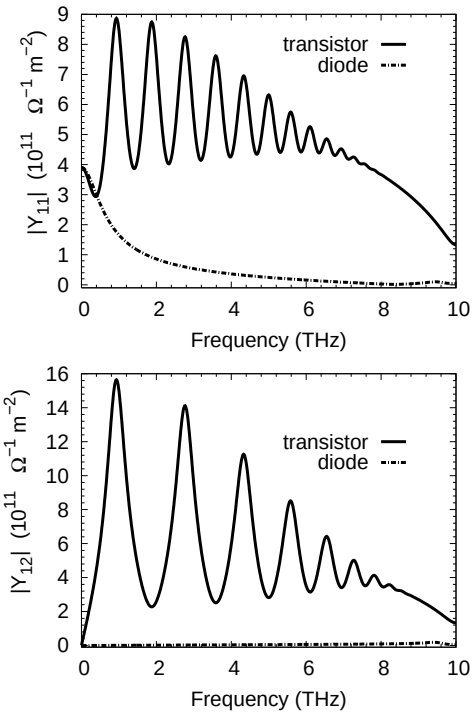

Figure 2: The admittance modulus $|Y_{ij}|$ calculated for the transistor and diode. With L = 400 nm, $n_0 = 8\times10^{17}$ cm^3, $\nu = 3\times10^{12}$ s^1, d = 10 nm for the transistor and $d \longrightarrow \infty$ for the diode.

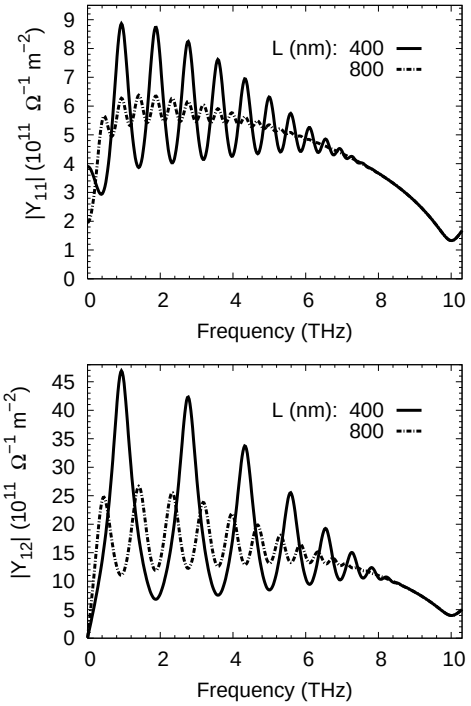

Figure 3: Frequency dependence of the transistor admittance modulus $|Y_{ij}|$ calculated for different channel lengths L. With $\nu = 3\times10^{12}$ s^1 and d = 10 nm.

uniform excitation along the channel cannot stimulate even modes.

For the case of diode ($d \longrightarrow \infty$), we observe that the appearance of the resonance peaks decreases when the gate effect becomes less and less evident (when the gate is moved). In addition, the diode behavior tends to suppress the resonance peaks due to the change of plasma wavelength by the form $\lambda = \sqrt{\epsilon_d/\epsilon_d d\delta}$. In this case, the resonance of the diode is proportional to free carrier plasma frequency $\omega_{res} = \omega_p$ (the resonance is related to the concentration n_0).

4.2 Device Length Effect

The figure 3 presents the dependence of the transistor admittance to the channel length L.

We remark that increasing the channel length modifies the frequency position and the quality of the resonances. Indeed, the resonances become less evident and more resonances appear in the same frequency range when the channel length increases to 800 nm. Physically, the resonance frequencies is inversely proportional to the channel length ($\omega_{res} \propto \frac{1}{(k+L)}$), this means, that the doubling of the channel length reduces by one half the resonance frequencies as clearly seen by comparing the continuous with the dashed lines in Fig. 3.

Figure 4 presents the dependence of the admittance on the channel length variation in the InGaAs diode when we consider the distance channel-gate tends to infinity ($d \longrightarrow \infty$).

We observe that the admittance exhibits a resonance peak at 9 THz and 8 THz for the channel length 400 nm and 800 nm respectively. However, an increasing of the channel length to 800 nm leads to increase the sharpness of the resonance peaks.

By considering ungated transistor ($d \longrightarrow \infty$), its effect on the channel weakens and the longitudinal term in Poisson equation $\frac{\partial^2 \Delta\varphi(x)}{\partial x^2}$ becomes stronger relatively to the transverse term $\beta\Delta\varphi(x)$, leading to weaker resonances at higher frequencies.

4.3 Relaxation Rate Effect

In this section, we investigate the small-signal response of the transistor terminals for two relaxation rate values 2×10^{12} and 3×10^{12} s^{-1}. The relaxation rate is related to the mobility μ through the relation $\nu = q/m^*\mu$ where m^* is the effective masse. The electron mobility as well as the relaxation rate depends strongly on the temperature. The figure 5 illustrates the frequency behavior of the small-signal admittance response for the relaxation rate values

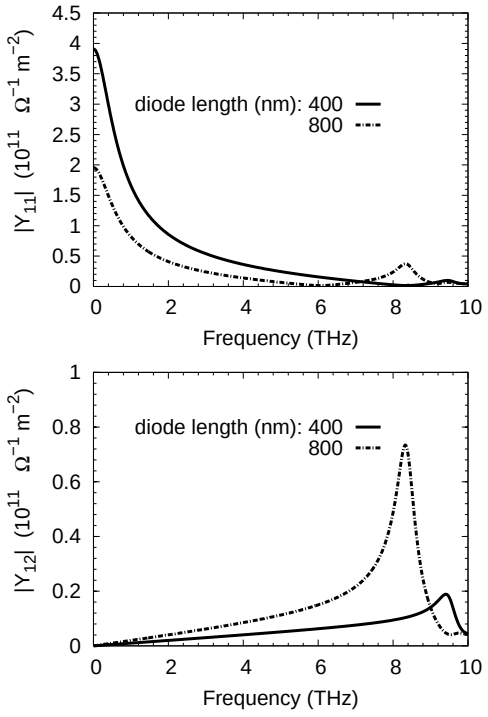

Figure 4: Frequency dependence of the diode admittance $|Y_{ij}|$ calculated for different diode length. With $\nu = 3{\times}10^{12}$ s^1 and $d \longrightarrow \infty$.

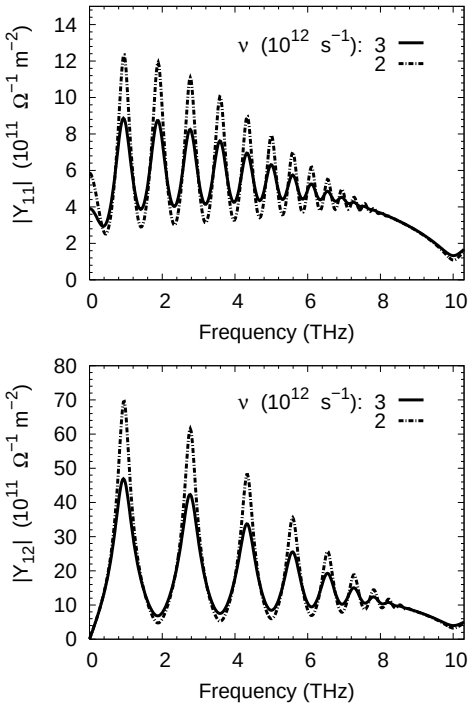

Figure 5: Frequency dependence of the transistor admittance modulus $|Y_{ij}|$ calculated for different relaxation rate value. With d = 10 nm and L=400 nm.

$3{\times}10^{12}$ and $2{\times}10^{12}$ s^{-1} corresponding to 300 and 200 K, respectively.

The low relaxation rate $2{\times}10^{12}$ s^{-1} increases the quality of the resonance without introducing modification of the periodic oscillations of the peaks.

The figure 6 presents the admittance behavior of the InGaAs diode for two relaxation rate $3{\times}10^{12}$ and $2{\times}10^{12}$ s^{-1}.

The low relaxation rate, on one hand, increases the admittance spectrum in low frequency and, on the other hand, increases the resonance peak near 9 THz. The transistor admittance spectrum presents a high oscillation compared to diode admittance.

4.4 Noise Spectrum

The noise spectrum is evaluated for the InGaAs transistor and unipolar diode by using equation (9). The figure 7 presents the current spectral density of drain and cathode in left and right of the figure respectively.

The current spectrum in figure 7 is calculated for $i = 1$ in equation (9) and by using the admittance Y_{11} at moderate temperature 300 k. The results of figure 7 (figure right) are similar to that calculated by the hydrodynamic equations in Ref [4]. We observe that the spectral current density exhibits resonance peaks corresponding to the plasma oscillations in the chan-

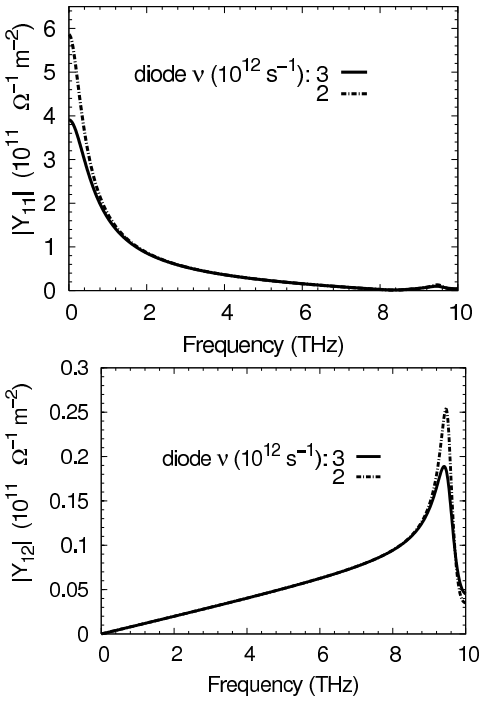

Figure 6: Frequency dependence of the diode admittance modulus calculated for different relaxation rate value. With d $\longrightarrow \infty$ and L=400 nm.

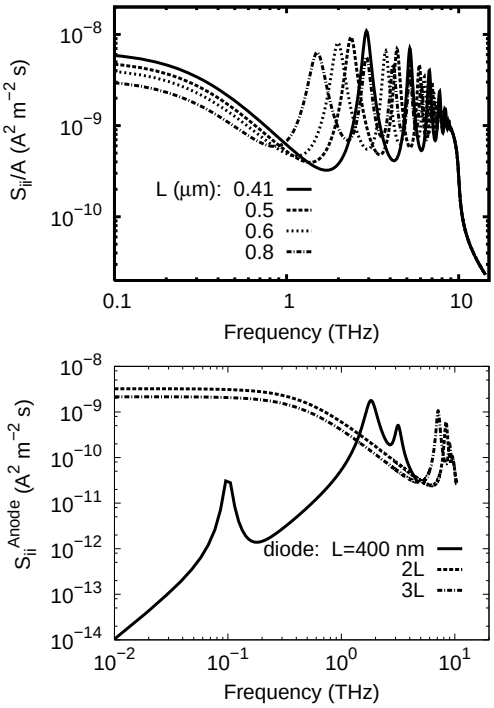

Figure 7: Spectral density of drain current fluctuations evaluated for different length values L. With $d = 10$ nm for the transistor, $d \longrightarrow \infty$ and $L = 400$ nm.

nel. The resonances in figure 7 are similar to that appeared in the admittance curve and depends on the channel length by ω_{res} form. Therefore, the length effect on the current spectrum curve is discussed before for the admittance in figure 3. The increasing of the length channel increases the number of the resonance due to the increasing of the free carrier plasma frequency (ω_p). For the diode with $L = 400$ nm, the spectral current density exhibits an initial growth proportional to ω^2 followed by two resonant peaks in the low and high frequency regions corresponding to the hybrid plasma resonance frequency (the appearance of homojunction). The appearance of the resonance peaks in the InGaAs diode is discussed in Ref [10].

5 Conclusion

We have investigated the small-signal response of the HEMT transistor and the homogenous diode (ungated transistor) in the THz range by using an analytical model. The approach takes into account the physical description of the drift carrier along the channel and the higher distance channel-gate supposition for the transistor and diode characterization, respectively. The drain admittance takes all the plasma resonances of fundamental excitation corresponding to $k = 0$, 1, 2, 3, 4.. while the gate and the drain-gate admittances present only the odd resonances. The behavior of the 2D electron gas in the transistor tends to the one of an ungated plasma, this leads to the appearance of a one resonance for the diode admittance spectrum. An increase of the channel length from 400 to 800 nm increases the oscillation and the number of the resonances in the devices. In addition, the decreasing of the relaxation rate to 2×10^{12} s^{-1} introduces an increasing of the resonance amplitude without modification on the frequency position of the peaks. Moreover, the noise spectral density exhibits a series of resonance peaks for the transistor and less resonance when we neglect the gate effect (case of diode). The series resonance peaks demonstrates that, in the frequency range from one to 10 THz, the transistor is more efficiency for the detection compared to the diode. Therefore, the discussion of the noise results can give significant information about the devices as detectors in high frequency.

Acknowledgements: The research was supported by the University of Montpellier, France in the case of the second author.

References:

[1] Fatima Zohra Mahi, Hugues Marinchio, Christophe Palermo and Luca Varani, *IEEE Transactions on Terahertz Science and Technology*. 5, 4 (2015).

[2] P. Shiktorov, E. Starikov, V. Gruzinskis, L. Varani, G. Sabatini, H. Marinchio and L. Reggiani, *Journal of Statistical Mechanics: Theory and Experiment*. DOI 10.1088/1742-5468/2009/01/01047 (2009).

[3] P. Shiktorov, E. Starikov, V. Gruzinskis, L. Varani, L. Reggiani, *Acta Physica Polonica.* 119 (2011).

[4] H. Marinchio, G. Sabatini, C. Palermo, J. Torres, L. Chusseau and L. Varani, *Journal of Physics: Conference Series*, 193 (2009) 012076.

[5] Fatima Zohra Mahi and Luca Varani, *International Journal of Mathematical, Computational*, 8, 2 (2014).

[6] J. P. Nougier, *IEEE Trans. Electron Devices*, 41 (1994) 2034.

[7] S. M. Sze, Physics of Semiconductor Devices, *Hoboken: Wiley-Interscience*, 1969.

[8] M. Shur, GaAs Devices and Circuits, *New York, London: Plenum press*, 1989.

[9] E. Starikov, P. Shiktorov and V. Gruzinskis, *Semiconductor Science and Technology*, 27 (2012) 045008.

[10] F. Z. Mahi, A. Helmaoui, L. Varani, P. Shiktorov, E. Starikov and V. Gruzinskis, *Journal of Physics IOP Publishing*, 193 (2009).